# 100 Gb/s SSB MB-OFDM metropolitan networks employing memory polynomials for SSBI mitigation

Gonçalo A. Martinho

***Abstract*—In this dissertation, it is assessed the performance of a system employing a 100 Gbit/s single sideband (SSB) multi-band orthogonal frequency division multiplexing (MB-OFDM) signal. This SSB signal, used to neglect the effect of the chromatic dispersion induced power fading (CDIPF) is created on the dual-parallel Mach Zehnder modulator (DP-MZM). The system uses direct-detection (DD) at the receiver, in which the distortion signal-signal beat interference (SSBI) is originated. With the use of memory polynomials (MP), it is evaluated if this performance issue can be mitigated, determining the required optical-signal-noise ratio (OSNR) that achieves a bit error rate of $10^{-3}$.**

**Two MB-OFDM systems were considered. The first one was designed to singly evaluate the performance improvement achieved by the MP. In this noise free single-band system, it was achieved an improvement of approximately ~7 dB on the system EVM. On the second system, both electrical and optical noise, SB and MB were considered, as well as the use of a nonlinear band selector and optical fibre. The configurations tested varied from ideal band selector and B2B configuration to a more realist system employing a nonlinear band selector, 2nd order super Gaussian model, and optical fibre, standard single-mode fibre (SSMF) model. This was meant to determine the minimum required OSNR to achieve a BER of $10^{-3}$. Despite the improvement of EVM achieved on the first test, the second showed a decrease in system EVM, caused primarily by the system MB configuration. It showed also the impossibility to achieve the BER of $10^{-3}$.**

***Index Terms*—multi band orthogonal frequency division multiplexing, dual-parallel Mach-Zehnder modulator, single side band, direct detection, positive intrinsic negative, signal-signal beat interference, memory polynomials.**

## I. Introduction

THE data traffic transferred over the telecommunication networks has increased during the last few years. The telecommunication networks are composed by the long-haul core, metropolitan (metro) and access networks. The metro (metropolitan) network is the interface between the core and the access networks. Therefore, it is responsible for transporting data between access networks and, when needed, transporting data to the core network. Since metro networks are responsible for processing all the traffic between the core and the access networks, it needs to be prepared to be highly flexible and scalable; it also needs to be able to reconfigure dynamically and, since the cost envisioned to these networks is reduced, the power consumption and the space occupied by the network elements also represent a constraint.

Along the years, the wavelength division multiplexing (WDM) technique has provided accommodation for the increasing traffic demand. However, it does not support higher levels of granularity than the provided by a single optical channel. Therefore, there is the need for new techniques that would enable the routing with granularity at the sub-wavelength level in future transparent metro networks.

Orthogonal frequency division multiplexing (OFDM) has been recently referred as an advantageous modulation format to provide high-speed optical transmission and capacity granularity. This happens because of its high spectral efficiency and its resilience in the presence of fibre dispersion and PMD [1-2]. Therefore, it represents a great solution to mitigate inter-symbol interference (ISI), which is caused by a dispersive channel [1]. This is very important because, since data rates are increasing, serial modulation schemes like quadrature amplitude modulation (QAM) are used, and so, the received signal depends on multiple transmitted symbols [3].

Although the OFDM systems are complex, the basic concept is simple [4-5]. Data is transmitted in parallel on a different number of frequencies, which are chosen to be mathematically orthogonal over one OFDM symbol period. As a result, the OFDM symbol period is longer than the one in the serial system, maintaining the same total data rate. Since the symbol period is longer, ISI affects less symbols, which simplifies equalization. To remove the residual ISI, most OFDM systems use a form of guard interval called cyclic prefix. Thanks to the almost rectangular shape of the OFDM optical spectrum, multiple OFDM signals can be transmitted without guard band between them [6].

To reduce the cost and to increase power efficiency of the next generation access networks, network operators presented a solution of integrating the metro and access networks in a single hybrid optical network [7-8], commonly known as long-reach passive optical network (LR-PON). Also, direct detection (DD) ought to be used. In DDO-OFDM, the optical carrier is sent along with the OFDM signal. With this, it is only needed a photodiode to perform the conversion from optical to electrical. But, with the usage of a photodiode a distortion arises during

the conversion from optical-to-electrical domain. This distortion is called the signal-signal beat interference (SSBI).
To mitigate the effect of the SSBI on the system, digital post distortion employing memory polynomials (MP) have been appointed. To mitigate the distortion SSBI, which is originated at a transmission channel, *S*, a digital post distorter with memory, based on memory polynomials (MPs) [9-12] is intended to implement an inverse system of *S* and then compensate the nonlinearities. The advantage of using MP-methods is the flexibility to adapt on real-time to variations of the parameters of system *S*.

This paper is structure as follows. In section II, the principles of MB-OFDM are presented. The DD system is described and the SSBI is introduced. Also, the MB-OFDM system parameters are presented. In section III, the SSBI mitigation technique used on this work, the MPs, is studied and characterize. In section IV, it is assessed the performance of the MB-OFDM system developed in this work. Finally, in section V, the conclusions of this report are presented.

## II. PRINCIPLES OF MB-OFDM

This dissertation is performed under the scope of the MORFEUS project [13]. The main objective of this project is to implement a metro network based on high data-rate MB-OFDM signals employing direct detection. This represents a great solution to provide, simultaneously, high flexibility in capacity allocation, high spectral efficiency and the possibility of upgrading the network capacity without changing the system architecture.

### *A. Basic principles of OFDM*

OFDM belongs to the multicarrier group, the type of modulation that carries information data through many low rate subcarriers. Classical MCM uses non-overlapped band-limited signals and needs a bank containing a large number of oscillators and filters at both transmitter and receiver [14-15], requiring excessive bandwidth. But with OFDM, the concept of orthogonality between sub-carriers grant an high-spectral efficiency during transmission, proposed in [14].

The block diagram of an OFDM transmitter and receiver is represented in figure II.1.

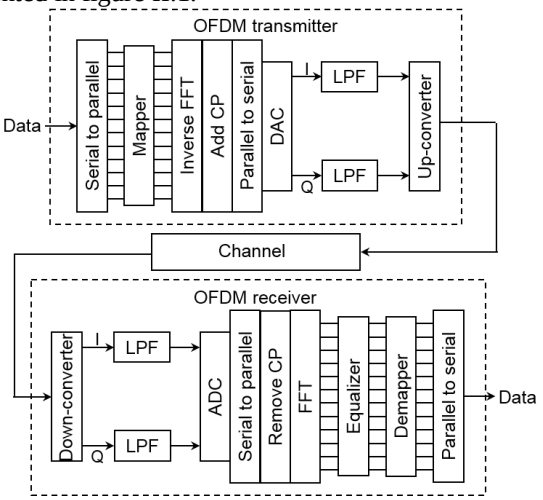


Figure II.1 - OFDM block diagram.

Starting at the transmitter, the OFDM signal is created in the following sequence:

- The input bit serial stream enters the serial to parallel converter (S/P) where it is splitted into $N_{sc}$ parallel bit streams;
- Then each of these bit streams is mapped into a symbol stream using for example an M-ary quadrature amplitude modulation (M-QAM);
- Afterwards, the recently mapped symbols enter the inverse fast Fourier transform (IFFT) where they are converted into an OFDM symbol stream;
- To prevent occurrence of inter-symbol interference (ISI) and inter-carrier interference (ICI) the cyclic prefix is added to each one of the OFDM symbols;
- Then, at the parallel to serial (P/S) converter, the OFDM symbols are converted to a serial data stream, in which the I/Q components of the signal are separated into independent channels. After that, these components are converted from digital to the analogue form at the digital-to-analogue converter (DAC);
- While being in independent channels, after converted to analogue, each I/Q component is filtered (filter with the bandwidth of the OFDM signal), in order to attenuate or remove the distortions created by the DAC.
- At last, the I/Q components enter the up-converter where they are combined and up-converted to the carrier frequency, in order to generate the OFDM signal that will be sent to the channel.

When the OFDM signal reaches the receiver, its process is the same of the transmitter but backwardly, with the addition of a single-tap equalizer block next to the FFT. The equalizer uses training symbols to estimate the channel characteristic, in order to compensate the distortion caused by the transmission channel.

The bitrate of an OFDM signal can be given by

$$R_b = \frac{N_{sc}}{T_s}\log_2 M \tag{1}$$

where $T_s$ represents the OFDM symbol period, $N_{sc}$ the number of subcarriers and M the number of different symbols of the modulation scheme. The bandwidth ($B_w$) of an OFDM signal can be given by

$$B_w = \frac{N_{sc}}{T_s} \tag{2}$$

With (1) and (2), the bitrate can be calculated using the signal bandwidth, given by

$$R_b = B_w \times \log_2 M; \tag{3}$$

### *B. DDO MB-OFDM*

In chapter 1, it was introduced the direct-detection optical OFDM system. The key feature of a DDO-OFDM is that it only needs a photodetector at the receiver, which is less expensive and complex when compared to the CO-OFDM system. However DD systems are impaired by chromatic dispersion induced power fading (CDIPF). Figure II.2 A represents the signal at the input and output of the PIN photodetector, where it is illustrated the effect of the CDIPF. This power fading appears because of the destructive beat between the two

sidebands, which is caused by the square law characteristic of the PIN and caused by the accumulated chromatic dispersion of the fibre link.

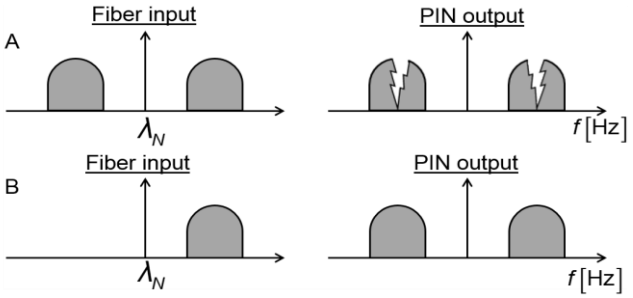


Figure II.2 - Illustration of the CDIPF effect on (A) the double sideband OFDM signal and (B) the SSB OFDM signal.

To overcome the CDIPF, there are two techniques that may be used, single side band (SSB) transmission and optical dispersion compensation. The SSB technique consists in transmitting only one of the two sidebands, making it possible to avoid the beat interference at the PIN (represented in figure II.2 B). The other technique is used to remove all the chromatic dispersion in order to avoid the destructive beat between the two sidebands. The main difference between these techniques is the part of the system where they are implemented. While SSB is implemented at the transmitter, optical dispersion compensation involves installing blocks of dispersion compensating fibre through the fibre link. Nowadays, network operators are working on moving all the network design to the transmitter and receiver's side, in order to leave the fibre links intact. So, if an upgrade is developed, it is no longer necessary to modify the fibre links. Therefore the SSB technique is more suitable. SSB OFDM has been widely proposed alongside systems employing DDO-OFDM. These SSB DDO-OFDM systems require a frequency gap between the optical frequency carrier and the OFDM signal. The frequency gap has usually the same width as the OFDM signal bandwidth and it is necessary to accommodate the distortion induced by the SSBI term generated by the photodetector.

The creation of a SSB-OFDM signal can be achieved by using an optical filter. However, the usage of an optical filter has several disadvantages, for instance, loss of power in the optical carrier, distortion on the remaining sideband, cross-talk caused by the residual sideband and reduced spectral efficiency, caused by the gap between the optical carrier and the OFDM information sideband, required for a correct filtering of the residual sideband. Another device capable of creating the SSB-OFDM signal, that does not suffer from the disadvantages listed above, is the dual-parallel Mach-Zehnder modulator (DP-MZM), proposed in [16]. The structure of the DP-MZM is represented in the figure II.3 and consists in a MZM with a MZM inserted in each arm. Since MZMs are composed by two parallel phase modulators, then this leads to a four phase-modulator structure.

After the SSB-OFDM signal is created, it travels through the optical fibre, which adds chromatic dispersion. When it reaches the receiver's end, the signal is converted from optical to the electrical domain in the photodetector, usually a PIN. The

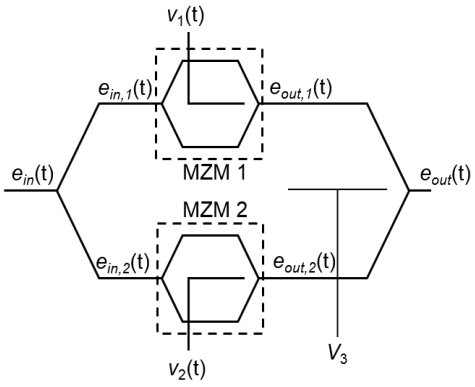


Figure II.3 - Illustration of a DP-MZM.

following deduction shows how the SSBI appears. After the photodetection, the PIN output current $i_{pin}$ (t) is given by

$$i_{pin}(t) = R_\lambda \times p_{pin}(t) \quad (4)$$

where $p_{pin}$(t) is the optical power of the incident optical signal and $R_\lambda$ the PIN responsivity. In this situation, the instantaneous power of an optical signal at the PIN input is given by

$$p_{pin}(t) = \left|e_{pin}(t)\right|^2 \quad (5)$$

where $e_{pin}$(t) is the optical field at the PIN input. To maintain the simplicity of this deduction, the output of the E/O is considered to be directly connect to the PIN input. Therefore, the optical field at its input is given by

$$e_{pin}(t) = A + Bs(t) \quad (6)$$

where A is a constant proportional to the optical carrier, B is a constant that depends on the switching voltage applied to the DP-MZM and $s$(t) is the OFDM signal from equation 2.1. Using equation 6 on 4 and considering that A and B are real, we obtain

$$i_{pin}(t) = R_\lambda . \left|e_{pin}(t)\right|^2 = R_\lambda \left[A^2 + 2ABs(t) + B^2 s^2(t)\right]. \quad (7)$$

In equation 7, the first term is the DC component $A^2$, the first order component 2ABs(t) is the received OFDM signal and the second order component $B^2$s2(t) is a nonlinear product, also known as signal-signal beat interference (SSBI), that may induce degradation on the detected electrical OFDM signal at the receiver end. In figure II.4, it is an illustration of the SSBI distortion.

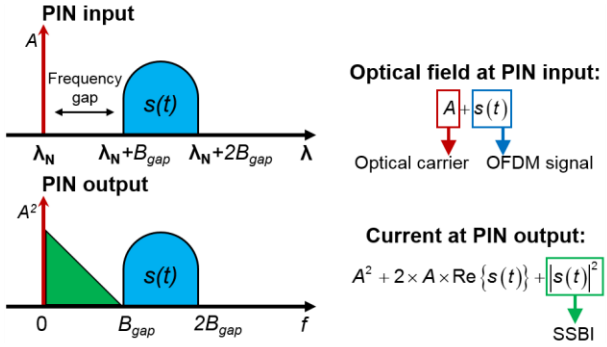


Figure II.4 - Illustration of the SSBI distortion.

Multiband-OFDM uses multiple bands instead of a single-band, more specifically, it is based on the division of a WDM channel (chj) into several independent OFDM sub-bands (bi,j) [17]. Each one of these sub-bands is an independent OFDM signal with its own optical carrier (FCij), as shown in figure II.5.

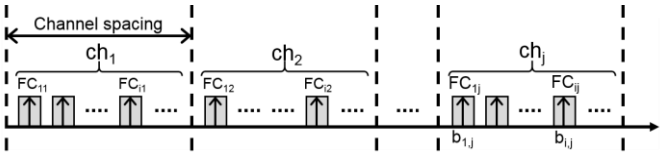


Figure II.5 - Optical spectra of MB-OFDM.

The signal used in the MORFEUS network is represented in figure 6. This MB-OFDM signal uses virtual carriers close to each OFDM band to assist in the detection process of that band.

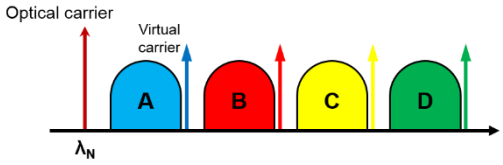


Figure II.6 - SSB MB-OFDM optical signal with virtual carriers used in MORFEUS network.

Despite the fact that the MORFEUS signal uses virtual carriers to aid in the detection of each OFDM band, the SSB MB-OFDM signal represented in figure II.6 also includes the optical carrier. The optical carrier may be needed to feed the electro-optic modulator of each node and to ensure relaxed constraints caused by laser phase noise and laser wavelength drift.

The MB-OFDM signal from figure II.6 is composed by several bands. The central frequency of each band is related with the central frequency of the other bands through the equation (considering that all OFDM bands have the same bandwidth):

$$f_{c,n} = f_{c,n-1} + \Delta f = f_{c,n-1} + BG + B_w, \quad n \in \{2,\ldots,N_B\} \quad (8)$$

where $f_{c,n}$ represents the central frequency of the $n$-th band, $N_B$ is the total number of bands, $BG$ is the gap between consecutive bands, $B_w$ is the bandwidth of the OFDM band and $\Delta f$ is the band spacing (which in this system is 3.125 GHz). Figure II.7 represents the parameters of equation 8.

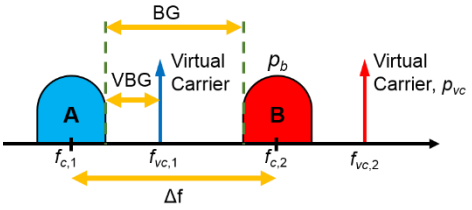


Figure II.7 - Illustration of the parameters that describe the OFDM bands of a MB-OFDM signal employing virtual carriers.

Figure 7, shows also the virtual carrier of each OFDM band. The frequency of each virtual carrier depends on the band gap between the OFDM band and the frequency of the virtual carrier. This band gap is the virtual band gap (*VBG*) and the frequency of the virtual carrier is given by:

$$f_{vc,n} = f_{c,n} + \frac{B_w}{2} + VBG, \quad (9)$$

where $f_{vc,n}$ is the virtual carrier frequency of the $n$-th band. Both OFDM band and virtual carrier are characterized by a power, in which $p_b$ is the power of the OFDM band and $p_{vc}$ is the power of the virtual carrier. These two powers are related through the virtual carrier-to-band power ratio (VBPR) given by

$$vbpr = \frac{p_{vc}}{p_b}. \quad (10)$$

The signal used on this work is, as mention before, an MB-OFDM signal, so its bitrate is composed by the bitrate of its bands. This bitrate, $R_{b,MB\text{-}OFDM}$, is given by

$$R_{b,MB-OFDM} = \sum_{n=1}^{N_B} R_{b,n} \quad (11)$$

where $R_{b,n}$ is the bitrate of the $n$-th OFDM band, which can be calculated through equation 12. Considering that all OFDM band parameters are the same, then the MB-OFDM signal bitrate can be simplified to

$$R_{b,MB-OFDM} = N_B R_b \quad (12)$$

where $R_b$ is the bitrate of a OFDM band.

Additionally, another parameter that describes the MB-OFDM signal used is its bandwidth. The MB-OFDM signal bandwidth is defined by:

$$B_{w,MB-OFDM} = \sum_{n=1}^{N_B} B_{w,n} + \sum_{i=1}^{(N_B-1)} BG \quad (13)$$

where $B_{w,n}$ is the bandwidth of each OFDM band, which can be calculated through equation 2.

### C. MB-OFDM system parameters

The system described in this work is designed for a bitrate of 100 Gbit/s and 16-QAM modulation. The target BER is $10^{-3}$, which is can be lowered to $10^{-15}$ thanks to the use of FEC with overhead of 12 % [18, 19]. Therefore, the target bitrate increases to 100 * 1.12 = 112 Gbit/s.

Since this MB-OFDM system is designed to have a channel spacing of 50 GHz with only 75% being used and the OFDM bans are spaced by a $\Delta f$ of 3.125 GHz, the number of OFDM bands that can be used are 12.

Therefore with 112 Gbit/s target bitrate and 12 OFDM bands, the bitrate per OFDM band becomes 9.33 Git/s. Using equation 2.35 this results in an OFDM bandwidth of 2.33 GHz and an OFDM signal period of 54.86 ns.

## III. Digital Post Distorter Employing Memory Polynomials

### A. MP theory

The MP used on this derives from a discrete version of the Volterra series [9]

$$y[n] = \sum_{p=1}^{P} \sum_{q_1=0}^{a_p} \cdots \sum_{q_p=0}^{a_p} h_p(q_1, q_2, \ldots, q_p) \prod_{m=1}^{p} x[n - q_m] \quad (14)$$

where $x[n-q_m]$ represents the input signal $x[n]$ delayed by $q_m$ samples, $y[n]$ represents the samples of the output signal and $h_p(q_1,q_2,\ldots,q_p)$ the Volterra kernel coefficients. According to [20], a simplified model of the memory polynomial is given by

$$\begin{aligned} y(n) = & \sum_{k_a=1}^{K_a}\sum_{q_a=0}^{Q_a} w_a \cdot x^{k_a}(n-q_a) + \\ & + \sum_{k_b=1}^{K_b}\sum_{q_b=0}^{Q_b}\sum_{m_b=1}^{M_b} w_b \cdot x(n-q_b)\cdot x^{k_b}(n-q_b-m_b) + \\ & + \sum_{k_c=1}^{K_c}\sum_{q_c=0}^{Q_c}\sum_{m_c=1}^{M_c} w_b \cdot x(n-q_c)\cdot x^{k_c}(n-q_c+m_c) \end{aligned} \quad (15)$$

where $w_a$, $w_b$ and $w_c$ represent the Volterra kernel coefficients $h_p(q_1,q_2,\ldots,q_p)$, $x(n)$ the input signal and $K_a$, $Q_a$, $K_b$, $Q_b$, $M_b$, $K_c$, $Q_c$ and $M_c$ the parameters of the MP, more specifically, $K_a$, $K_b$ and $K_c$ indicate the order of the MP and the rest indicates the delays applied to the input signal x. The number of coefficients, $N_C$, that compose the memory polynomial represented in 15 can be calculated through expression 16

$$N_C = K_a\cdot(Q_a+1) + K_b\cdot(Q_b+1)\cdot M_b + K_c\cdot(Q_c+1)\cdot M_c \quad (16)$$

in which $K_a\cdot(Q_a+1)$ represent the coefficients that belong to the signal where the delays applied are the same, equal to $q_a$; $K_b\cdot(Q_b+1)\cdot M_b$ the coefficients that represent the lagging terms of signal x in which the delays are of different durations, being the first delay $q_b$ and the second $q_b+m_b$ and $K_c\cdot(Q_c+1)\cdot M_c$ give the coefficients that represent the leading terms of signal x. In this case the delays are also different, but although the first one is equivalent to the previous case, $q_c$, the second delay is $q_c-m_c$. The delays represent the memory of the MP. This means that when a MP has a high delay, it has an high memory, leading to a MP that can compensate more dispersive effects, with the cost of computer simulation.

The coefficients **w**, (*w* is composed by the coefficients $w_a$, $w_b$ and $w_c$), are obtained by estimation. This estimation is performed in three steps: (1) capturing $N_S$ samples from the input and output signals, *x* and *y*, respectively; (2) creating the matrix **V** from the sampled signal *y*, and finally, (3) calculating the vector **w** (which contains the coefficients *w*) from matrix **V** and the sampled input signal **x**, through expression 17 [9]

$$\begin{cases} \mathbf{w} = \left(\mathbf{V}^{\mathrm{H}}\mathbf{V}\right)^{-1}\mathbf{V}^{\mathrm{H}}\cdot\mathbf{x} = \mathbf{V}^{-1}\cdot\mathbf{x} \\ \mathbf{x} = \left[x[1], x[2], \ldots, x[N_S]\right]^T \end{cases}. \quad (17)$$

where $(.)^T$ denotes the transpose operation and $(.)^H$ the complex conjugate transpose operation. The matrix **V**, referred in step (3), is a matrix with $N_S$ rows and $N_C$ columns. To facilitate the understanding on how matrix **V** is composed, it can be considered that matrix **V** has three inner matrixes, one for each component of the memory polynomial presented in 15,

$$\mathbf{V} = \left[\mathbf{V}_A \quad \mathbf{V}_B \quad \mathbf{V}_C\right]. \quad (18)$$

The matrix **V** can then be calculated through expression 19

$$\mathbf{V}_A = \begin{bmatrix} y^{k_a}[1-q_a] \\ \vdots \\ y^{k_a}[N_S-q_a] \end{bmatrix}$$

$$\mathbf{V}_B = \begin{bmatrix} y[1-q_b]\,y^{k_b}[1-q_b-m_b] \\ \vdots \\ y[N_S-q_b]\,y^{k_b}[N_S-q_b-m_b] \end{bmatrix} \quad (19)$$

$$\mathbf{V}_C = \begin{bmatrix} y[1-q_c]\,y^{k_c}[1-q_c+m_c] \\ \vdots \\ y[N_S-q_c]\,y^{k_c}[N_S-q_c+m_c] \end{bmatrix}$$

The memory polynomial presented in expression 15 is implemented in the digital signal processor (DSP). The DSP is located at the receiver, after the PIN photodetector, as it is represented in figure III.1.

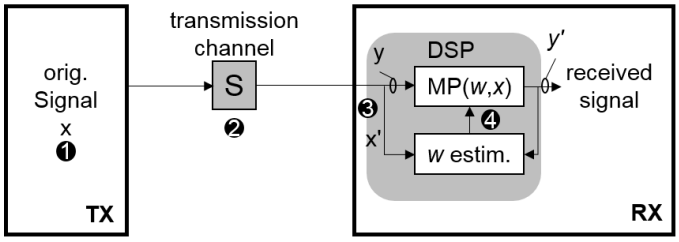


Figure III.1 - Location of the DSP on the MB-OFDM system.

Since the DSP is located at the receiver, this MP implementation is called digital post-distortion. The SSBI mitigation process using the MP from expression 15 is:

1 – The OFDM signal is created at the transmitter and it is composed by the training symbols and information symbols.

2 – The OFDM signal enters the optical modulator (DP-MZM in this work) and its output enters the transmission channel (optical fibre). At the receiver, it passes through the band selector (2nd order super Gaussian filter) and is photodetected in the PIN, passing from the optical to the electrical domain.

3 – The received electrical signal then enters the DSP where the transmitted signal x is reconstructed using the training symbols. Using the reconstructed signal x' and the samples from the received signal corresponding to the training symbols, the coefficients of the MP are estimated.

4 – With the coefficients and the complete received signal, the signal without the effect of the SSBI is created and used for processing.

### *B. Determination of the best MP structure*

To determine the best structures of the MP that were able to mitigate the SSBI, a test that returned approximately 204000 results was executed. The system considered in this test was noise free and its parameters are represented in table III.1. The first half of the signal x was used to estimate the coefficients because it corresponds to the samples of the training symbols, which are known.

Table III.1 - System parameters used on the tests executed.

| Parameter | Value |
|---|---|
| Number of subcarriers | 128 |
| Number of OFDM symbols | 200 |
| Number of OFDM training symbols | 100 |
| Number of samples per chip | 32 |
| Sampling mode | S&H |
| Number of samples $N_s$ | 528000 |
| Number of OFDM bands | 1 |
| Binary rate of each band [Gbit/s] | 10 |
| OFDM symbol period [ns] | 51.2 |
| Cyclic prefix [ns] | 12.8 |
| Number of subcarriers | 128 |
| Central frequency of the 1st band [GHz] | 2 |
| OFDM band bandwidth [GHz] | 2.5 |
| VBG [MHz] | 90 |
| Modulation order | 16QAM |

This test comprised 6 use-cases, in which the MP is composed by a certain summation of the complete structure from expression 15. The uses-cases were the 1st summation, the 2nd summation, the 3rd summation, the 1st and the 2nd summations (referred from now on as the past MP), the 1st and 3rd summations (referred from now on as the future MP) and the complete MP.

Having chosen the cases that were going to be assessed, it had to be chosen the structures of the MP that were to be tested. It was decided that the order of the MP should not be higher than 5 and the delays should not be more than 5. Before the test was executed, the starting EVM of the system without any mitigation for the SSBI was -10.5 dB. The constellation at the receiver with no SSBI mitigation is represented in figure 8 in blue and with ideal SSBI mitigation in orange.

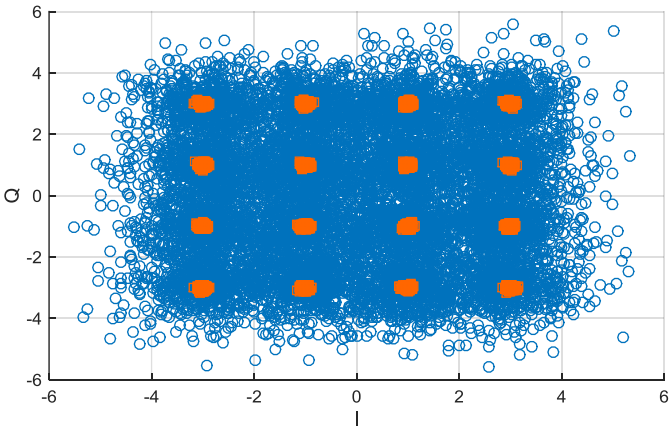


Figure III.2 - Constellation at the receiver when no SSBI mitigation is used (blue) and when SSBI ideal mitigation is used (small orange dots).

After obtaining the results, it was executed a preliminary analysis, in which it was concluded that the first three cases defined earlier were not important to consider because the EVM values obtained were the same as the beginning or worse. The second analysis made to the latter three cases (past MP, future MP and complete MP) was intended to find the structures that were able to achieve the better system performance, without taking into account the number of coefficients required. It was always considered at least one structure of each case (the past, future and complete MP) in order to compare and evaluate if the three components of the MP shown in expression 15 were important or if one of them could be discarded. The structures that were chosen in this second analysis are presented in table III.2.

In table III.2, there are represented the memory polynomial structures that presented the best performance improvement. It is also represented the number of coefficients that each structure requires to achieve that performance improvement.

Table III.2 - Results after second analysis.

| $K_a$ | $Q_a$ | $K_b$ | $Q_b$ | $M_b$ | $K_c$ | $Q_c$ | $M_c$ | EVM [dB] | $N_C$ |
|---|---|---|---|---|---|---|---|---|---|
| Past MP structure | | | | | | | | | |
| 4 | 4 | 4 | 4 | 5 | 0 | 0 | 0 | -16.69 | 120 |
| Future MP structure | | | | | | | | | |
| 2 | 3 | 0 | 0 | 0 | 4 | 4 | 5 | -16.98 | 108 |
| Complete MP structure | | | | | | | | | |
| 1 | 4 | 4 | 4 | 5 | 4 | 2 | 4 | -17.01 | 153 |

In the third analysis, the number of coefficients required by each MP structure was taken into account when deciding which of the structures was considered to be the better relation between performance achieved (EVM value) and complexity required (coefficients). To perform this analysis, it was considered a starting structure for the past and future MP and then each parameter ($K_a$, $Q_a$, $K_b$, $Q_b$, $M_b$, $K_c$, $Q_c$ and $M_c$) was altered to see how the EVM value and coefficient number would vary. The approach used to perform the third analysis on the complete MP was different. Since the complete MP had 200000 different possibilities, it was impossible to analyse by altering the MP parameters one by one. Therefore it was used a different approach. The 200000 possibilities were divided into groups. These groups contained only structures with an achieved EVM lower than -16.5 dB. The parameter used to divide the possible structures into groups was the number of coefficients used, for example, the first group was for structures that used between 70 and 79 coefficients, and so on.

After dividing by groups it was concluded that the EVM of MPs with a number of coefficients between 70 and 79 were around -16.5 dB. When the coefficients were between 80 and 89, there was a case that achieved a value of EVM inferior to -16.5 dB and was the lowest compared to the others in that same group. This case which is represented in table III.3.

Table III.3 - Best structures for the MPs considered.

| $K_a$ | $Q_a$ | $K_b$ | $Q_b$ | $M_b$ | $K_c$ | $Q_c$ | $M_c$ | EVM [dB] | $N_C$ |
|---|---|---|---|---|---|---|---|---|---|
| Past MP structure | | | | | | | | | |
| 2 | 4 | 4 | 4 | 5 | 0 | 0 | 0 | -16.70 | 110 |
| Future MP structure | | | | | | | | | |
| 2 | 2 | 0 | 0 | 0 | 4 | 4 | 5 | -16.96 | 106 |
| Complete MP structure | | | | | | | | | |
| 3 | 4 | 4 | 1 | 5 | 4 | 1 | 4 | -16.76 | 87 |

Also, in figure III.3 it is represented the constellation at the receiver when the complete MP is used and in figure III.4 the spectrum of the received signal after the SSBI is mitigated by the complete MP. Marked in red is the DSP input signal with

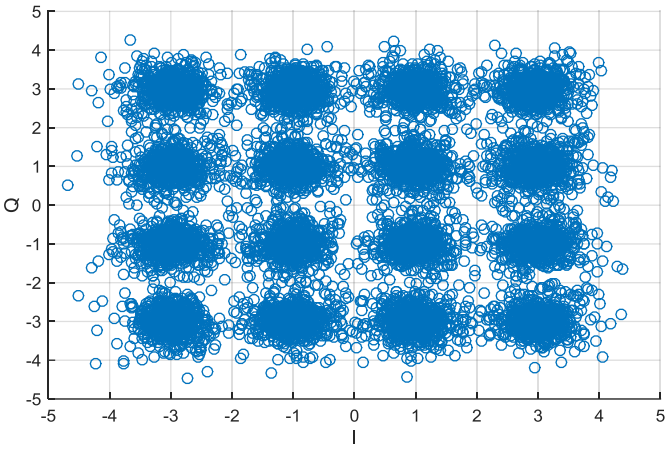


Figure III.3 - Constellation at the receiver when the complete MP is used to mitigate SSBI.

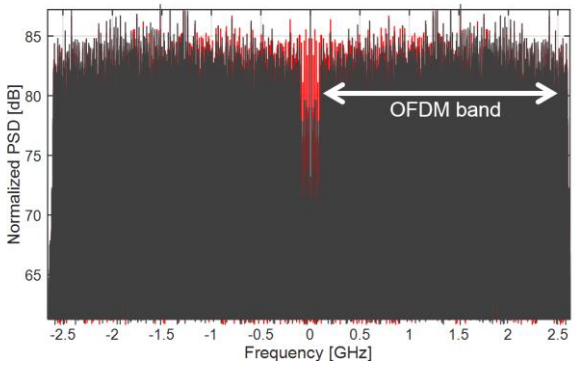


Figure III.4 - Spectrum at the DSP output. The spectrum on the back (red) is at the DSP input. On top (grey) is the spectrum at the DSP output.

SSBI and in black the signal with the SSBI mitigated by the MP.

In table III.3, the best structures of MP are presented. Each one of them uses a large quantity of coefficients, which increases the computer complexity of the system. In order to reduce this complexity, each structure was tested with the objective of determining if all the coefficients of the same structure were important. . In this test, each coefficient, one by one, was forced to zero and then the value of the EVM was calculated, in order to determine if that coefficient was important or if it could be discarded. Figure III.5 represent the results of this test, for the complete MP structure.

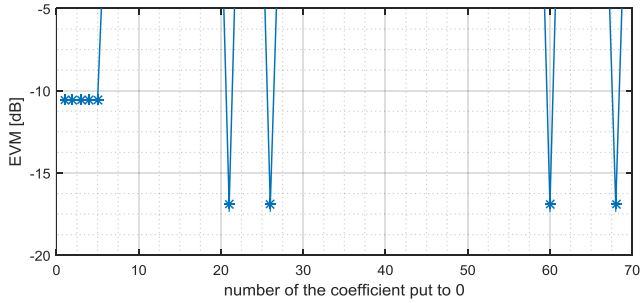


Figure III.5 - Assessment of the importance of the coefficients of the complete MP.

Figure III.5 shows that the coefficients from the complete MP structure are all important. This conclusion is verified by the fact that when each coefficient is forced to zero, the EVM instead of being approximately equal to the values presented in table 2 for the complete MP, became approximately -10 dB for the initial coefficients and 2 dB for the rest of them. This test was done for the past and future MP and the result was similar.

### *C. Adaptive iteration method*

In previous test, the performance achieved was obtained with a certain sequence of OFDM symbols that originated an optimal value for the coefficients estimated. However, when random sequences of OFDM symbols are used, the coefficients obtained are different from the optimal and therefore the performance obtained is not the same. Although the MP structures chosen can achieve acceptable performance results when random symbols are used, the randomness of the OFDM symbols sometimes result in cases of poor performance. This problem occurs because the coefficients of the MP are estimated based on the part of the signal that corresponds to the training symbols and the EVM is calculated using the information symbols. If the coefficients were to be estimated based on the information symbols, then the performance of the system would increase significantly. To try and solve this problem, a technique proposed in [9] was used which relies on the update of the coefficients. Since the structure of the MP cannot be changed, the coefficients of the MP have to be updated in order to withstand the different OFDM symbols sequences that are used in the system. This update can be done through an adaptive technique as it is proposed in [9] and the values of ($i$+1)-th estimate of $\mathbf{w}$ are given by

$$\mathbf{w}_{i+1} = \mathbf{w}_i + \mu \cdot \left(\mathbf{V}^{\mathrm{H}}\mathbf{V}\right)^{-1}\mathbf{V}^{\mathrm{H}}\left(\mathbf{u} - \mathbf{V}\mathbf{w}_i\right) \qquad (20)$$

where $\mu$ is the relaxation constant. The update performed on the coefficients with the expression 20 is achieved by calculating the error between the signal from the transmitter x and the approximation that is calculated through $\boldsymbol{Vw_i}$, where $\boldsymbol{V}$ is the matrix from expression 19 and $\boldsymbol{wi}$ are the coefficients from the previous iteration. This error is then multiplied with $\left(\mathbf{V}^{\mathrm{H}}\mathbf{V}\right)^{-1}\mathbf{V}^{\mathrm{H}}$, which is $\mathbf{V}^{-1}$, in order to obtain the value of the coefficients associated to the error. This correction value is then multiplied with the relaxation constant and then summed to the value of the previous coefficients. This operation is intended to be executed one time, each time the input OFDM symbol sequence changes and the value of the relaxation constant, according to [9], $\mu$ has to be inferior to one. Choosing the value of this constant has two possible outcomes. On one hand, if the value is big, then the coefficients would rapidly converge to the optimal value, but this would lead to an unstable convergence because, since the μ value is big, the coefficient values would vary too much, which could also lead to no convergence at all. On the other hand, if the μ value is small, the unstable problem of the high value of μ would not occur, but the convergence would be slower. The typical value used, according to [9] is 0.1.

In order to conclude which would be the optimum value for the relaxation constant, each MP structure was tested for a μ between 0 and 0.1.

The reason why this extensive test depicts that the best value for μ is 0 is because of the first 200 OFDM symbol sequence.

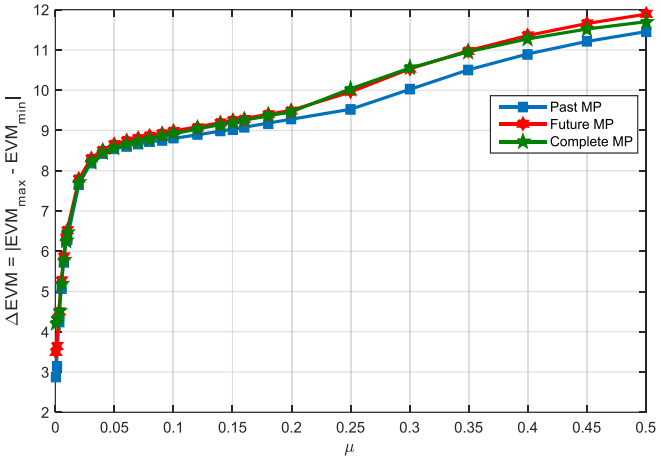


Figure III.6 - EVM variation between maximum and minimum value for each relaxation constant value.

Since the first sequence is similar to the optimum sequence from table III.3, the coefficients don't need any update at all. With the increase of the μ value, the coefficients values deviate from there optimum value, which leads to an increase on the difference of EVM. This last test helped however to understand that the behaviour of the three MPs is similar, so the past and future MPs were discarded. To help determine the optimum relaxation constant, the complete MP was tested several times, each starting at a different OFDM symbol sequence. In figures III.7 and III.8 these results are displayed. Also, in each figure it is represented a line for the BER without the use of adaptive. The line on top is obtained estimating the coefficients with the training symbols. The line on bottom is obtained using the information symbols on the coefficient estimation.

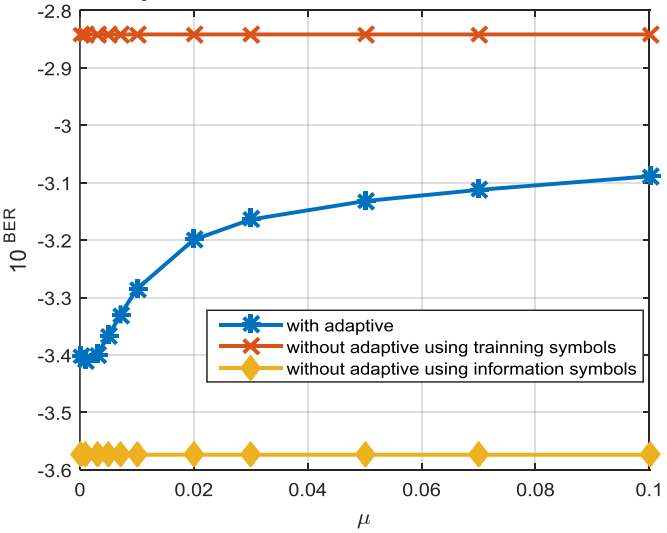


Figure III.7 - , BER obtained for the original OFDM symbol sequence as the first one.

When looking at these 2 cases obtained by calculating the mean BER value, the conclusion is that when the first sequence is similar to the optimal (figure III.7), the use of adaptive with μ=0 increases the value obtained for the BER. When the first sequence is not similar to the original one (figure III.8), the use of adaptive with μ > 0 tends to reduce the BER achieved. In both cases, the increase on BER or decrease on BER is not significant. Therefore, the use of adaptive with μ > 0 does not bring any advantage. It tends to add computer complexity, without improving the BER signal when compared to the case without adaptive. So the choice is to adaptive with μ = 0, which means that the coefficients used on the first estimation stay untouched.

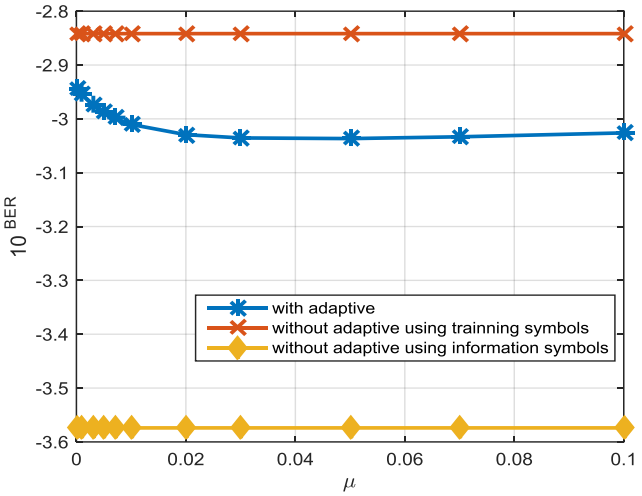


Figure III.8 - , BER obtained for a random OFDM symbol sequence as the first one.

## IV. MB-OFDM SYSTEM PERFORMANCE EVALUATION

The main objective of this work is the mitigation of the SSBI distortion. However, there are other sources of distortion present on the MB-OFDM system, like the electrical-to-optical modulator (the DP-MZM in this work), the band selector (2nd order super Gaussian model) and the transmission medium (SSMF optical fibre).

This evaluation is supported by the determination of the EVM and BER values for each band of the MB-OFDM system. The BER is calculated using the exhaustive Gaussian approach (EGA), which allows its value to be estimated using different values of noise, increasing the accuracy of the results. With these calculations, it is determined if it is possible to achieve a BER of $10^{-3}$ and if doing so, what is the minimum required optical signal-to-noise ratio (OSNR).

To determine this minimum required OSNR, four different evaluations were conducted, each one focusing on the impact of a non-linear component present on the MB-OFDM system. As introduced in the beginning of this chapter, the non-linear components considered were the 2nd order super Gaussian filter used on the band selector and the SSMF optical fibre used in the transmission channel.

The tests were performed using a SB system and MB system. Each system was designed using the parameters described in section II.C and table III.1 except for the OFDM

symbol period which was the one from II.C. Also in this system electrical and optical noise were considered. Regarding the 2nd order super Gaussian filter, the BS bandwidth was equal to the bandwidth of the group OFDM band plus VBG, the central frequency of 2.2 GHz and detuning of 300 MHz were defined according to [21]. In case of the SSMF fibre, the lengths considered were 100 kms, 200 kms, 300 kms and 400 kms.

Table IV.1 - Results for 2nd order super Gaussian band selector with SSMF model (Lf=100km), SB.

| SB, Lf = 100 km | |
|---|---|
| OSNR [dB] | 33.75 |
| 10BER | -1.88 |
| EVM [dB] | -15.69 |

Table IV.2 - Results for 2nd order super Gaussian band selector with SSMF model (Lf=100km), MB.

| MB, Lf = 100 km | | | | | | |
|---|---|---|---|---|---|---|
| Band | 1 | 2 | 3 | 4 | 5 | 6 |
| OSNR [dB] | 39.25 | 36.75 | 39.5 | 33.25 | 40 | 35 |
| $10^{BER}$ | -1.75 | -2.19 | -1.67 | -1.81 | -2.16 | -1.94 |
| EVM [dB] | -14.5 | -14.3 | -13.8 | -14.1 | -14.0 | -12.4 |
| Band | 7 | 8 | 9 | 10 | 11 | 12 |
| OSNR [dB] | 40 | 39.5 | 40 | 37 | 39 | 39.5 |
| $10^{BER}$ | -1.85 | -2.1 | -2.15 | -2.08 | -2.02 | -2.7 |
| EVM [dB] | -10.1 | -14.4 | -14.3 | -13.4 | -14.8 | -15 |

After presenting the results obtained for the case fibre length 100 kms, which represent the best case scenario in terms of optical fibre length. The first one and the more important is the fact that it is not possible to achieve the BER of $10^{-3}$, defined in the objectives. The values for OSNR represented on table IV.1 and IV.2 are the ones that achieve the lowest BER. This could have been caused by the non-linearity from the electrical to optical modulator used in this work, the DP-MZM; by the incapability of the MP to mitigate the SSBI or also caused by simulation errors.

Aside the fact that the objective was not achieved, there was also another value that was not expected, which was the value for the BER of the SB and MB in each case. It was expected that the BER for the SB case, since there is no crosstalk present or harmonics from other bands, would be lower than the MB values, which did not occur. This occurrence could not be explained.

Apart from these results, an effect that was verified on the results obtained was the distortion present in each band being different. For example, bands 1 and 12 were supposed to be the bands with better performance results since are the less affected by crosstalk or harmonics from the other bands. Between these two the 12th band was the one that presented the best values as expected, because during selection the filter would select a small part of the next band. Since this was the last band it cased less distortion in the photodetection process. As expected as well, the bands 6 and 7, being the bands from the middle of the MB-OFDM signal, were the most affected by distortion caused by crosstalk and harmonics of the other bands of the MB-OFDM signal.

## V. Conclusion

In this work, the study of a 100 Gbit/s SSB MB-OFDM metropolitan system employing DP-MZM and MP for SSBI mitigation was performed. Additionally, the study and characterisation of the MP theory as a SSBI mitigation technique was presented and implemented on the system. It was concluded that the system (SB or MB configuration) presented was not able to achieve a BER of $10^{-3}$.

## References


[1] A. Lowery, L. Du, and J. Armstrong, "Orthogonal frequency division multiplexing for adaptive dispersion compensation in long haul WDM systems," *Conf. on Optical Fiber Communication*, Anaheim, CA, USA, March 2006, pp.1-3.

[2] S. Jansen, I. Morita, and H. Tanaka, "10x121.9-Gb/s PDM-OFDM transmission with 2-b/s/Hz spectral efficiency over 1,000 km of SSMF," *Conf. on Optical Fiber Communication*, San Diego, CA, USA, February 2008.

[3] J. Armstrong, "OFDM for optical communications," *J. Lightw. Technol.*, vol. 27, no. 3, pp. 189-204, February 2009.

[4] J. Bingham, "Multicarrier modulation for data transmission: An idea whose time has come," *IEEE Commun. Mag.*, vol. 28, no. 5, pp. 5-14, May 1990.

[5] W. Zou and Y. Wu, "COFDM: An overview," *IEEE Trans. Broadcast.*, vol. 41, no. 1, pp 1-8, March 1995.

[6] R. Dischler and F. Buchali, "Transmission of 1.2 Tb/s continuous waveband PDM-OFDM-FDM signal with spectral efficiency of 3.3 bit/s/Hz over 400 km of SSMF," *Conf. on Optical Fiber Communication*, San Diego, CA, USA, March 2009, pp. 1-3.

[7] R. Davey, D. Grossman, M. Wiech, D. Payne, D. Nesset, A. Kelly, A. Rafael, S. Appathurai, and S. Yang, "Long-reach passive optical networks," *J. Lightw. Technol.*, vol. 27, no. 3, pp. 273-291, February 2009.

[8] N. Cvijetic, M. Huang, E. Ip, Y. Huang, D. Qian, and T. Wang, "1.2Tb/s symmetric WDM-OFDM-PON over 90km straight SSMF and 1:32 passive split with digitally-selective ONUs and coherent receiver OLT," *Conf. on Optical Fiber Communication*, Los Angeles, CA, USA, March 2011, pp.1-3.

[9] D. Morgan, Z. Ma, J. Kim, M. Zierdt, and J. Pastalan, "A generalized memory polynomial model for digital predistortion of RF power amplifiers," *IEEE Trans. Signal Process.*, vol. 54, no. 10, pp. 3852-3860, October 2006.

[10] L. Ding, G. Zhou, D. Morgan, M. Zhengxiang, J. Kenney, J. Kim, and C. Giardina, "A robust digital baseband predistorter constructed using memory polynomials," *IEEE Trans. Commun.*, vol. 52, no. 1, pp. 159–165, January 2004.

[11] Z. Liu, M. Violas, and N. Carvalho, "Digital predistortion for RSOAs as external modulators in radio over fiber systems," *Optics Express*, vol. 19, no. 18, pp. 17641–17646, August 2011.

[12] Y. Pei, K. Xu, J. Li, A. Zhang, Y. Dai, Y. Ji, and J. Lin, "Complexity-reduced digital predistortion for subcarrier multiplexed radio over fiber systems transmitting sparse multi-band RF signals," *Optics Express*, vol. 21, no. 3, pp. 3708–3714, February 2013.

[13] T. Alves, L. Mendes, and A. Cartaxo, "High granularity multiband OFDM virtual carrier-assisted direct-detection metro networks," *J. Lightw. Technol.*, vol. 33, no. 1, pp. 42-54, November 2014.

[14] Y. Liu, J. Zhou, W. Chen, and B. Zhou, "A robust augmented complexity-reduced generalized memory polynomial for wideband RF power amplifiers," *IEEE Trans. Ind. Electron.*, vol. 61, no. 5, pp. 2389–2401, June 2013.

[15] T. Alves, J. Morgado, and A. Cartaxo, "Linearity improvement of directly modulated PONs by digital pre-distortion of coexisting OFDM-based

signals," in *Advanced Photonics Congress*, Colorado Springs, CO, USA, June 2012, pp. 1-2.
[16] R. Mosier and R. Clabaugh, "Kineplex, a bandwidth-efficient binary transmission system," *AIEE Trans.*, vol. 76, no. 6, pp. 723-728, January 1958.
[17] M. Zimmerman and Alan L. Kirsch, "The AN/GSC-10 (KATHRYN) variable rate data modem for HF Radio," *IEEE Trans. Commun. Technol*, vol. 15, no. 2, pp. 197-204, April 1967.
[18] J. Armstrong, "Analysis of new and existing methods of reducing intercarrier interference due to carrier frequency offset in OFDM," *IEEE Trans. Commun.*, vol. 47, no. 3, pp. 365-369, March 1999.
[19] W. Peng, B. Zhang, F. Kai-Ming, X. Wu, A. Willner. and C. Sien, "Spectrally efficient direct-detected OFDM transmission incorporating a tunable frequency gap and an iterative detection techniques," *J. Lightw. Technol.*, vol. 27, no. 24, pp. 5723-5735, October 2009.
[20] G. Agrawal, Fiber-Optic Communication Systems, 3rd edition, Wiley-Interscience, USA, 2002.
[21] ITU-T G.975.1, Forward Error Correction for high bit-rate DWDM Submarine System, February 2004.
[22] ITU-T G.709/Y.1331, Interfaces for the optical transport network, February 2012.
[23] J. Morgado, "Linearization of directly modulated lasers," Internal Report, Instituto de Telecomunicações, Lisboa, January 2012.
[24] T. Alves and A. Cartaxo, "Virtual Carrier-Assisted Direct-Detection MB-OFDM Next-Generation Ultra-Dense Metro Networks Limited by Laser Phase Noise," *J. Lightw. Technol.*, vol. 33, no. 19, pp. 4093-4100, August 2015.